Chinese Chemical Letters 33 (2022) 3026–3030

Contents lists available at ScienceDirect

Chinese Chemical Letters

journal homepage: www.elsevier.com/locate/cclet

Probing and modulating the interactions of the DNAzyme with DNA-functionalized nanoparticles

Yuqiang Hu[a], Zhen Zhang[a], Wei Zhang[b,c], Minghao Hu[a], Xianjin Xiao[b], Tongbo Wu[a,*]

[a] School of Pharmacy, Tongji Medical College, Huazhong University of Science and Technology, Wuhan 430030, China
[b] Institute of Reproductive Health/Center of Reproductive Medicine, Tongji Medical College, Huazhong University of Science and Technology, Wuhan 430030, China
[c] Department of Obstetrics and Gynaecology, Union Hospital, Tongji Medical College, Huazhong University of Science and Technology, Wuhan 430022, China

ARTICLE INFO

Article history:
Received 14 July 2021
Revised 11 August 2021
Accepted 9 September 2021
Available online 15 September 2021

Keywords:
Gold nanoparticles
DNAzyme
Interface interaction
Rate difference
Human apurinic/apyrimidinic endonuclease 1

ABSTRACT

DNA-functionalized gold nanoparticles are one of the most versatile bionanomaterials for biomedical and clinical diagnosis. Herein, we discovered that the performance of DNAzyme cleaving the substrate is highly related to its length. This intriguing phenomenon only appears at the interfaces of DNA-functionalized gold nanoparticles. We systematically investigated the causes of this phenomenon. We conjectured that the DNAzyme with extended nucleotides that do not match its substrate strand is vulnerable to non-specific adsorption, electrostatic repulsion, and steric hindrance. Based on our improved understanding of this phenomenon, we have successfully developed a highly sensitive and specific amplifiable biosensor to detect human apurinic/apyrimidinic endonuclease 1.

Gold nanoparticles (AuNPs) have been applied as sensors [1], diagnostic tools [2] and drug carriers [3] in many aspects of chemistry, biology and medicine. AuNPs could be stabilized by thiolates using the gold-sulfur (Au–S) bond [4]. Oligonucleotides, peptides and polyethylene glycol (PEGs) are easily attached to AuNPs in this way [5]. The terminal sulfhydryl modification (HS-) in the single-stranded DNA (ssDNA) is widely used to connect ssDNA with AuNPs to form DNA-functionalized AuNPs [3,6-8]. However, other involute interactions between ssDNA and AuNPs also exist. The interactions include non-specific adsorption [9], electrostatic repulsion [10], hydrophobic interactions [11] and specific bonding between the gold and chemical groups of purine and pyrimidine rings in DNA bases [12-15]. These interactions may affect the hybridization performance of oligonucleotides on functionalized AuNPs.

Many studies have pay attention to the covalent and non-covalent forces between ssDNA and AuNPs [16,17]. One category studied the interactions between ssDNA and bare AuNPs [18]. Another category focused on the HS-ssDNA functionalized AuNPs and studied the interactions between non-sulfhydryl bases in the HS-ssDNA and AuNPs [12,19-21]. However, few works investigated the interactions between HS-ssDNA functionalized AuNP and its corresponding analytes, such as functional nucleic acids. The interaction between the analytes and HS-ssDNA functionalized AuNPs may cause unexpected results when dealing with analytes holding different structures, limiting the application of AuNPs.

DNAzyme is a functional nucleic acid with several practical advantages compared with protein enzymes or ribozymes, including easy preparation, easy modification, high chemical and thermal stability [22,23]. Thus, DNAzymes often work as attractive, amenable and adaptable biocatalysts to amplify labels or reporter units, arousing the growing interest in many biosensing events [24-28].

In this work, we found that DNAzymes with various lengths behaved differently to cleave the HS-ssDNA substrate labelled on AuNPs. As DNAzymes with different lengths are widely utilized in solutions (without AuNPs) as molecular-recognition elements for various biosensing platforms [29,30], this phenomenon may impede their applications if one wants to combine these platforms with AuNPs. Thus, we systematically studied the effects of electrostatic repulsion, non-specific adsorption and steric hindrance on the DNAzyme as the analyte to react with the HS-ssDNA functionalized AuNPs. The results improved our understanding of the difference in DNAzyme cleavage rate at the AuNPs interface comparing with that in the solution. Furthermore, using the novel property of the DNAzyme, we successfully developed a highly sensitive and selective biosensor to detect human apurinic/apyrimidinic endonuclease 1 (APE1).

* Corresponding author.
E-mail address: wutongbo@hust.edu.cn (T. Wu).

https://doi.org/10.1016/j.cclet.2021.09.039
1001-8417/

Table 1
Part of oligonucleotide sequences used in this work.

Name	DNA sequence (5′-3′)
Probe-1	HS-$(T)_{14}$CACTAT/rA/GGAAGAGAT-FAM
Probe-2	BHQ-CACTAT/rA/GGAAGAGAT-FAM
DNAzyme-0	ATCTCTTCTCCGAGCCGGTCGAAATAGTG
DNAzyme-1	TAGAACCGAATTTGTGATCTCTTCTCCGAGCCGGTCGAAATAGTG
DNAzyme-2(5′T6)	TTTTTTATCTCTTCTCCGAGCCGGTCGAAATAGTG
DNAzyme-3(5′T16)	TTTTTTTTTTTTTTTTATCTCTTCTCCGAGCCGGTCGAAATAGTG
DNAzyme-4(3′biotin)	ATCTCTTCTCCGAGCCGGTCGAAATAGTG-biotin
DNAzyme-5(5′biotin)	biotin-ATCTCTTCTCCGAGCCGGTCGAAATAGTG

We used 8–17E DNAzyme as the model DNAzyme, which could cleave a substrate strand in the presence of the cofactor Mn^{2+} [31]. The substrate strand (marked as probe-1, see the sequence in Table 1) is a DNA-RNA chimeric sequence composed of an RNA nucleotide flanked by two DNA domains. These two DNA domains (green in Table 1) are binding regions of two arms of the DNAzyme and contain 6 and 9 nucleotides (nt), respectively. The probe-1 was conjugated to AuNP through its 5′-HS. AuNP would quench the 3′-carboxyfluorescein (FAM) fluorophore in probe-1 after the conjugation. We also added a 14-nt poly-thymine spacer in probe-1 to enhance its accessibility to the DNAzyme. After constructing the HS-ssDNA-functionalized AuNPs, TEM was used to characterize the bare and functionalized AuNPs (Figs. S1A and B in Supporting information). Both the bare and functionalized AuNPs were uniformly distributed in the solution with an average diameter of 20 nm. The absorption peak at 260 nm of DNA and redshifted characteristic peaks after functionalizing AuNPs with DNA proved that the substrate was successfully conjugated (Fig. S1C in Supporting information).

When reacting with the functionalized AuNPs, which were conjugated with hundreds of probe-1 strands, the DNAzyme could cleave a probe-1 strand, releasing two short fragments. Then, the DNAzyme would dissociate from the fragments to hybridize and cleave another probe-1 strand. When the FAM-labelled fragment departs from the surface of the AuNP, the fluorescent signal would be recovered. Therefore, the fluorescent signal will continue to increase during the DNAzyme cleavage, and the rate of fluorescence increase could reflect the cleavage rate of the DNAzyme.

As previously reported [31], the original 8–17E DNAzyme (marked as DNAzyme-0, see the sequence in Table 1) worked well to generate fluorescent signals using the above principle. In DNAzyme-0, the arms (the green part in the DNAzyme in Fig. 1 and Table 1) perfectly match probe-1. We added 16 extended bases that do not match probe-1 (the black part in the DNAzyme in Fig. 1 and Table 1) to the 5′-end of DNAzyme-0 to form DNAzyme-1 (see the sequence in Table 1). To our surprise, the fluorescent signal generated by DNAzyme-1 cleavage was significantly lower than that by DNAzyme-0.

To avoid the potential second structure forming in the longer DNAzyme with extended bases, we designed another two DNAzymes by adding 6 or 16 thymines at the 5′-end of DNAzyme-0 to obtain DNAzyme-2(5′T6) and DNAzyme-3(5′T16) (Fig. 2A). The fluorescent signals generated by DNAzyme-2 and -3 cleavage with AuNPs were also much lower than DNAyzme-0 (Fig. 2B). And the DNAzyme-3 with a longer 5′ length had a lower reaction rate. To exclude the influence of AuNPs, we added a small molecule quencher (BHQ-1) at the 5′-end of the DNAzyme substrate strand to form probe-2 (see the sequence in Table 1). In the intact probe-2, FAM is quenched by BHQ-1. After DNAzyme cleavage, FAM and BHQ-1 will depart from each other to release the fluorescent signal. As shown in Fig. 2C, the fluorescent signal generated by all the DNAzymes was similar when they reacted with probe-2 without

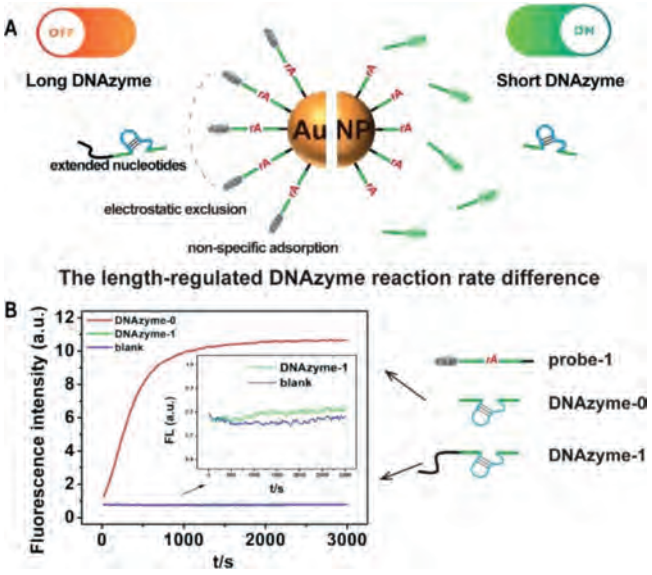

Fig. 1. (A) Schematic illustration of the phenomenon of the length-regulated DNAzyme reaction rate difference. (B) The fluorescence responses of the DNAzyme-0 and DNAzyme-1 to probes on AuNPs. The biosensor without any DNAzyme was used as the blank.

AuNPs. These results indicated that the length-regulated DNAzyme reaction rate difference might result from the interactions between HS-ssDNA functionalized AuNPs and DNAzymes.

Toward this difference, we first suspected that it was caused by electrostatic repulsion. Due to the polyanionic characteristic of the phosphate backbone, DNA is usually negatively charged [18]. AuNPs also tend to be negatively charged with the anion ligands around the surface of AuNPs [32]. Therefore, to achieve successful hybridization with probe-1, the DNAzyme must overcome electrostatic repulsion forces between the DNAzyme and functionalized AuNPs. The salt is often used to screen the charge repulsion [33]. In the above experiment, NaCl in the solution was 200 mmol/L. As the salt concentration gradually increased, the relative cleavage rates of DNAzymes-2 and -3 also gradually rise, and the relative cleavage rate of DNAzyme-2–5′T6 reaches the platform at 400 mmol/L (Fig. 2D and Fig. S2A in Supporting information). These results indicated that NaCl helped the longer DNAzymes overcome electrostatic repulsion forces. However, the cleavage rates of DNAzyme-2 and -3 only recovered to 58% and 44% of the cleavage rate of DNAzyme-0, even with 500 mmol/L NaCl (Fig. 2D and Fig. S2A). Therefore, electrostatic repulsion was not the only interaction between the DNAzyme and AuNPs.

Another possible interaction between the DNAzyme and AuNPs may be non-specific adsorption. Adsorption of the DNA bases on AuNPs could even inactivate the hybridization function of the DNA [34]. With extended nucleotides, the DNAzyme could be easier to

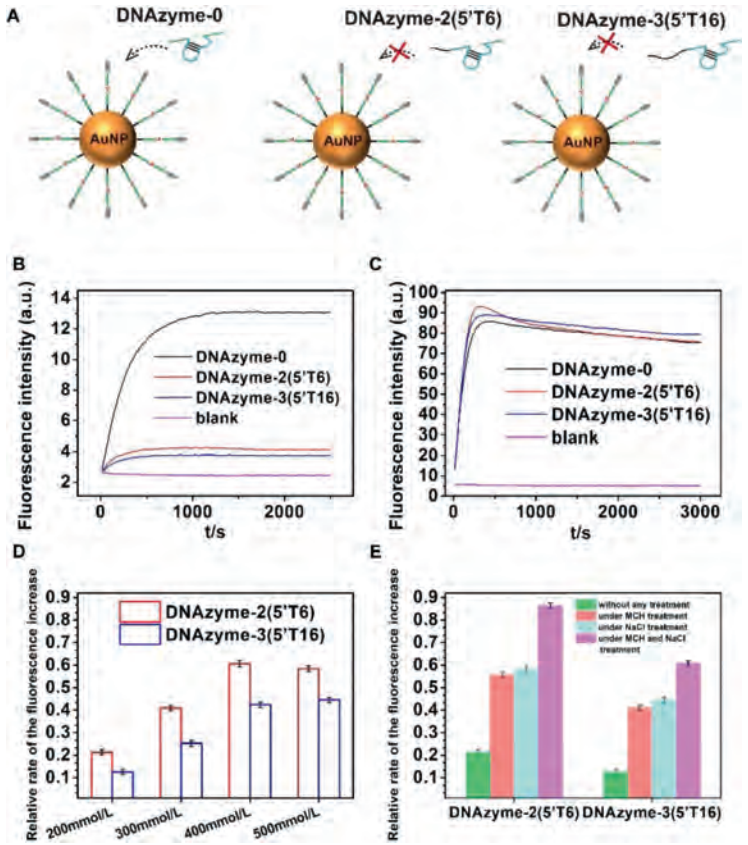

Fig. 2. (A) Schematic illustration of the three DNAzymes. (B) The fluorescence responses of the DNAzyme-2 and DNAzyme-3 to substrates on AuNPs. (C) The fluorescence responses of the DNAzyme-2 and DNAzyme-3 to substrates in solution. (D) The relative rates of fluorescence increase of the DNAzyme-2 and DNAzyme-3 with different NaCl concentrations. (E) The relative rates of fluorescence increase of the DNAzyme-2 and DNAzyme-3 with different treatment. The relative rate means the ratio of the fluorescence increase rate of each variant DNAzyme to DNAzyme-0 under the same conditions. The fluorescence responses of DNAzyme-0 under different conditions can be found in Fig. S2 (Supporting information). Error bars show the standard deviation of three experiments in all the figures.

be adsorbed by AuNPs. Thus, the longer DNAzyme cannot readily hybridize with probe-1 on AuNPs, resulting in a low cleavage rate. To confirm this hypothesis, we adopted a small-molecule blocking agent, 6-mercapto-1-hexanol (MCH), to block the adsorption site on AuNPs. As previously reported, an MCH monolayer on AuNPs could prevent the contact between the DNA bases and AuNPs [21,35,36]. Therefore, MCH treatment before adding the DNAzyme could minimize the influence of non-specific adsorption. The results showed that the relative cleavage rate of DNAzyme-2 and -3 increased about 2.61 and 3.27 times after MCH treatment (under MCH treatment v.s. without any treatment in Fig. 2D). We also tried to use NaCl treatment and MCH treatment at the same time. The cleavage rate of DNAzyme-2 and -3 increased about 4.1 and 4.8 times after MCH treatment (under MCH and NaCl treatment *vs.* without any treatment in Fig. 2E and Fig. S2B in Supporting information). At the same time, the relative cleavage rates of the DNAzyme-2 and -3 recovered to 86% and 61% under MCH and 500 mmol/L NaCl treatment.

HS-ssDNA functionalized AuNPs own a relatively high charge and create an electrostatic exclusion zone (Fig. S3 in Supporting information). The extended bases on the longer DNAzyme make them harder to get into the zone than DNAzyme-0. Even if a part of the longer DNAzyme gets into the exclusion zone by chance, non-specific adsorption will prevent them from generating fluorescent signals. For DNAzyme-0, the hybridization energy with the substrate strand is more significant than the adsorption energy with AuNPs. And DNAzyme-0 prefers to bind with the substrate. For the longer DNAzyme, the extended mismatched bases provide more adsorption sites and make the adsorption energy more significant than the hybridization energy. Thus, only a tiny part of longer DNAzymes could bind with the substrate strands and could not produce enough cleavage.

We also probed the steric effect by chemically modifying DNAzyme-0 with a biotin molecule at the 3′-end and 5′-end to form DNAzyme-4(3′biotin) and DNAzyme-5(5′biotin) (Fig. S4 in Supporting information). This biotin modification has little influence on the cleavage rate. Furthermore, a sizeable streptavidin (SA) was introduced through the strong streptavidin-biotin interaction to increase the steric hindrance. As shown in Fig. S4, DNAzyme-4(3′biotin) activity decreased more than a half compared with DNAzyme-0, and DNAzyme-5(5′biotin) activity did not change. As 3′-biotin is close to the surface of AuNPs and 5′-biotin is not, the results suggesting the steric hindrance on the surface of AuNPs will also affect the performance of DNAzyme. Thus, as the extended bases may cause more steric hindrance, the cleavage rate of longer DNAzyme may be affected. The influence of the probe density on AuNPs was also discussed in Fig. S5 (Supporting information).

The above results indicate that the length-regulated DNAzyme reaction rate difference is probably caused by electrostatic repulsion, non-specific adsorption and steric hindrance simultaneously. Once increasing the number of extended mismatched bases, non-specific adsorption, electrostatic repulsion and steric hindrance will dominate the interactions between the DNAzyme and HS-ssDNA functionalized AuNPs and prevent DNAzyme from working. Further verification and universality of the phenomenon were discussed in Figs. S6 and S7 (Supporting information), respectively.

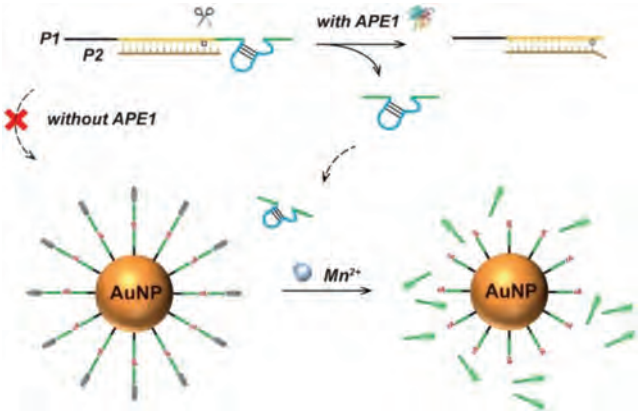

Fig. 3. Schematic illustration of rational design of the biosensor for APE1 detection.

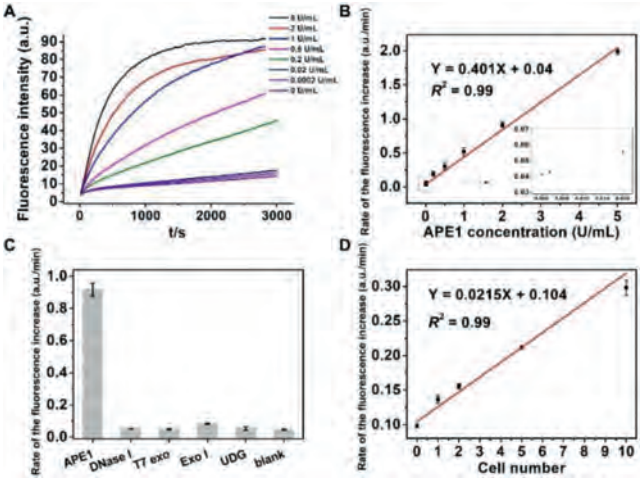

Fig. 4. (A) The fluorescence responses of the biosensor with APE1concentrations from 0 to 5 U/mL. (B) The linear relationship between the rate of fluorescence increase and the APE1 concentration. (C) The selectivity of the biosensor with to APE1 over other enzymes. The biosensor without any enzyme was used as the blank. (D) The linear relationship between the rate of fluorescence increase and the Hela cell number.

Our mechanistic model suggests that the effects of electrostatic repulsion, non-specific adsorption and steric hindrance on different analytes shall be considered when designing functionalized AuNPs-based biosensors or functional devices. Here, we demonstrate that our improved understanding of the interactions between AuNPs and the analyte could be used to design the biosensor for APE1 detection rationally.

APE1 plays a critical role in the base excision repair (BER) pathway of DNA lesions to maintain genome stability [37,38]. It is also involved in regulating cellular responses to oxidative stress conditions [39]. Abnormal expression/localization of APE1 has been found in tumour cells [40]. APE1 specifically incises the phosphodiester immediately 5′ to the apurinic/apyrimidinic site (AP site) in the double-stranded DNA (dsDNA) and generates a short DNA strand [41,42].

As shown in Fig. 3, the dsDNA substrate of APE1 was formed by **P1** and **P2. P1** consists of three regions. At **P1**'s 5′-end is the poly-T region composed of 14 T bases (black in Fig. 3). In the middle of **P1**, there is the dsDNA region (yellow) to hybridize with P2. The DNAzyme region is set at the 3′-end of **P1** (green). The AP site is designed between the dsDNA region and the DNAzyme region. **P2** can hybridize with **P1**'s dsDNA region to form a structure with two bases protruding from the AP site. As we previously reported [43], APE1 has the best activity on the substrate with this structure. The **P1**/**P2** duplex is vulnerable to non-specific adsorption, electrostatic repulsion and steric hindrance of the functionalized AuNPs due to the long poly-T and the rigid dsDNA region, resulting in a slow cleavage rate of the DNAzyme in **P1**/**P2**. In the presence of APE1, APE1 will digest the AP site and release the free DNAzyme (DNAzyme-0). The free DNAzyme could cleave the substrate strand on AuNPs to generate fluorescent signals. Thus, the rate of fluorescence increase reflects the amount of APE1. Agarose gel electrophoresis was carried out to verify the hybridization between **P1** and **P2** and the hydrolysis behaviour of APE1 to the **P1**/**P2**. In addition, agarose gel electrophoresis also confirmed our biosensor design with AuNPs for APE1 detection. A detailed discussion could be found in Fig. S8 (Supporting information).

Figs. 4A and B showed that the biosensor could rapidly respond to APE1 at different concentrations with a linear range from 0.0002 U/mL to 5 U/mL and the detection limit of the method was 0.0002 U/mL. It is more sensitive than most of the methods for APE1 detection. Our biosensor's high sensitivity could be attributed to the background suppression based on non-specific adsorption, electrostatic repulsion and steric hindrance without APE1 and the signal amplification of the functionalized AuNPs with free DNAzyme. Fig. 4C summarizes the selectivity of the biosensor for APE1 against other possibly coexisting nucleases. APE1 aroused a strong fluorescence response, and other enzymes with the same concentration as APE1 only generate a neglectable fluorescent signal. We further applied the proposed biosensor to measure endogenous APE1 in human cervical cancer cell lysates (HeLa cells). The cell lysate was obtained from about 10^6 HeLa cells/50 μL. We diluted the cell lysate with different folds to test the APE1 in the sample. We found that the fluorescence increase rate was highly related to the dilution fold (Fig. S9 in Supporting information), and it exhibited a linear correlation with the dilute fold from 4×10^5 to 4×10^4 (corresponding to 1 to 10 cells in the reaction system with 20 μL, Fig. 4D). Thus, the method can be used to detect APE1 in biological samples with a single-cell level.

HS-ssDNA functionalized AuNP is frequently used to assemble various DNA nanosensors or nanodevices. However, the interaction of the analyte with AuNPs has often been overlooked. In this work, we systematically probed the effects of non-specific adsorption, electrostatic repulsion, and steric hindrance on the DNA analyte by monitoring the cleavage rates of the DNAzymes with different lengths. The results revealed critical roles of non-specific adsorption, electrostatic repulsion, and steric hindrance, which should be carefully evaluated for designing and modulating AuNPs-based biosensors or functional devices. We also successfully adopted these findings to rationalize the design of amplifiable biosensors for biomarker detection. The designing and validating of the APE1 detection biosensor suggest that the improved understanding of the interaction between the analyte and HS-ssDNA functionalized AuNPs may promote the development of biosensors and nanodevices in the future.

Declaration of competing interest

The authors declare that they have no known competing financial interests or personal relationships that could have appeared to influence the work reported in this paper.

Acknowledgments

This work was supported by the National Natural Science Foundation of China (Nos. 82172372 and 21904045), COVID-19 Pneumonia Emergency Scientific Research Special Fund of Wuhan (No. EX20D03), and the Fundamental Research Funds for the Central Universities (Nos. 2019kfyXJJS169 and 2021yjsCXCY127).

Supplementary materials

Supplementary material associated with this article can be found, in the online version, at doi:10.1016/j.cclet.2021.09.039.

References

[1] T. Xiao, J. Huang, D. Wang, et al., Talanta 206 (2020) 120210.
[2] P. Singh, S. Pandit, V.R.S.S. Mokkapati, et al., Int. J. Mol. Sci. 19 (2018) 1979.
[3] M.E. Kyriazi, D. Giust, A.H. El-Sagheer, et al., ACS Nano 12 (2018) 3333–3340.
[4] M. Giersig, P. Mulvaney, Langmuir 9 (1993) 3408–3413.
[5] D.E. Cliffel, F.P. Zamborini, S.M. Gross, R.W. Murray, Langmuir 16 (2000) 9699–9702.
[6] T. Cui, J.J. Liang, H. Chen, et al., ACS Appl. Mater. Interfaces 9 (2017) 8569–8580.
[7] B. Li, Y. Liu, Y. Liu, et al., ACS Nano 14 (2020) 8116–8125.
[8] C.C. Chang, G. Wang, T. Takarada, M. Maeda, ACS Sens. 4 (2019) 363–369.
[9] P. Sandström, M. Boncheva, B. Åkerman, Langmuir 19 (2003) 7537–7543.
[10] H. Li, L. Rothberg, Proc. Natl. Acad. Sci. U. S. A. 101 (2004) 14036.
[11] E.M. Nelson, L.J. Rothberg, Langmuir 27 (2011) 1770–1777.
[12] L.M. Demers, M. Östblom, H. Zhang, et al., J. Am. Chem. Soc. 124 (2002) 11248–11249.
[13] M. Östblom, B. Liedberg, L.M. Demers, C.A. Mirkin, J. Phys. Chem. B 109 (2005) 15150–15160.
[14] H. Kimura-Suda, D.Y. Petrovykh, M.J. Tarlov, L.J. Whitman, J. Am. Chem. Soc. 125 (2003) 9014–9015.
[15] S. Piana, A. Bilic, J. Phys. Chem. B 110 (2006) 23467–23471.
[16] E. Boisselier, D. Astruc, Chem. Soc. Rev. 38 (2009) 1759–1782.
[17] J.M. Carnerero, A. Jimenez-Ruiz, P.M. Castillo, R. Prado-Gotor, ChemPhysChem 18 (2017) 17–33.
[18] K.M. Koo, A.A.I. Sina, L.G. Carrascosa, et al., Anal. Methods 7 (2015) 7042–7054.
[19] A.B. Steel, R.L. Levicky, T.M. Herne, M.J. Tarlov, Biophys. J. 79 (2000) 975–981.
[20] J. Yang, B.K. Pong, J.Y. Lee, H.P. Too, J. Inorg. Biochem. 101 (2007) 824–830.
[21] K.A. Brown, S. Park, K. Hamad-Schifferli, J. Phys. Chem. C 112 (2008) 7517–7521.
[22] D. Morrison, M. Rothenbroker, Y. Li, Small Methods 2 (2018) 1700319.
[23] M. Cepeda-Plaza, A. Peracchi, Org. Biomol. Chem. 18 (2020) 1697–1709.
[24] Y. Liao, S. Guo, X. Hua, et al., Sens. Actuators B 310 (2020) 127862.
[25] A.C. Zimmermann, I.M. White, J.D. Kahn, Talanta 211 (2020) 120709.
[26] K. Jiang, Y. Wu, J. Chen, et al., Chin. Chem. Lett. 32 (2021) 1827–1830.
[27] X. Shi, H.M. Meng, X. Geng, et al., ACS Sens. 5 (2020) 3150–3157.
[28] Y. Wu, H.M. Meng, J. Chen, et al., Chem. Commun. 56 (2020) 470–473.
[29] C. Zhang, J. Yang, S. Jiang, et al., Nano Lett. 16 (2016) 736–741.
[30] J. Pan, Y. He, Z. Liu, J. Chen, Chem. Commun. 57 (2021) 1125–1128.
[31] H. Peng, X.F. Li, H. Zhang, X.C. Le, Nat. Commun. 8 (2017) 14378.
[32] J. Liu, Phys. Chem. Chem. Phys. 14 (2012) 10485–10496.
[33] X. Zhang, M.R. Servos, J. Liu, Langmuir 28 (2012) 3896–3902.
[34] T.M. Herne, M.J. Tarlov, J. Am. Chem. Soc. 119 (1997) 8916–8920.
[35] R. Levicky, T.M. Herne, M.J. Tarlov, S.K. Satija, J. Am. Chem. Soc. 120 (1998) 9787–9792.
[36] D. Zhu, H. Pei, J. Chao, et al., Nanoscale 7 (2015) 18671–18676.
[37] S. Fang, L. Chen, M. Zhao, Anal. Chem. 87 (2015) 11952–11956.
[38] G. Li, J. Li, Q. Li, Nanoscale 11 (2019) 20456–20460.
[39] J. Zhai, Y. Liu, S. Huang, et al., Nucleic Acids Res. 45 (2017) e45.
[40] A.R. Evans, M. Limp-Foster, M.R. Kelley, Mutat. Res. DNA Repair 461 (2000) 83–108.
[41] M. Zhou, C. Feng, D. Mao, et al., Biosens. Bioelectron. 142 (2019) 111558.
[42] Y. Zhang, Y. Deng, C. Wang, et al., Chem. Sci. 10 (2019) 5959–5966.
[43] Y. Hu, Z. Zhang, W. Ye, et al., Sens. Actuators B 330 (2021) 129332.